Bull. Mater. Sci. (2018) 41:2
https://doi.org/10.1007/s12034-017-1516-8

Gd impurities effect on Co_2CrSi alloy: first-principle calculations

I E YAHIAOUI[1], A LAZREG[1,*], Z DRIDI[1], Y AL-DOURI[2,3] and B BOUHAFS[1]

[1]Modelling and Simulation in Materials Science Laboratory, Department of Physics, University of Sidi Bel-Abbes, 22000 Sidi-Bel-Abbes, Algeria

[2]Nanotechnology and Catalysis Research Center (NANOCAT), University of Malaya, 50603 Kuala Lumpur, Malaysia

[3]Department of Physics, Faculty of Science, University of Sidi-Bel-Abbes, 22000 Sidi-Bel-Abbes, Algeria

*Author for correspondence (aeklazreg@yahoo.fr)

MS received 17 June 2016; accepted 5 December 2017; published online 2 February 2018

Abstract. First-principle calculations have been performed to study Gd impurities doping effect on the physical properties of the Heusler half-metallic ferromagnet Co_2CrSi using the density functional theory in the local spin density approximation with an additional Hubbard correlation term for the rare-earth 4f states. The results show that the gadolinium moment is aligned antiparallel to that of transition metal atoms for both $Co_{16}Cr_7GdSi_8$ and $Co_{15}GdCr_8Si_8$. The analysis of the doped material band structures shows that the half-metallic properties are completely conserved if Gd substitutes Cr atoms, while the minority-spin gap is filled and half-metallicity is lost when Gd substitutes Co atoms.

Keywords. Half-metallic; spin polarization; Heusler alloys.

1. Introduction

Half-metallic ferromagnets have been intensively studied in the field of spintronics. In these compounds only one spin channel presents a gap at the Fermi level, while the other has a metallic character, leading to 100% carrier spin polarization at the Fermi energy (E_F) [1,2]. Therefore, since the first prediction of half-metallicity for the half-Heusler compound NiMnSb in 1983 [1], intensive research on half-metallic materials has been carried out [3–11]. Most of the Co-based full-Heusler compounds in the cubic $L2_1$ structure are ferromagnetic (FM) with a high Curie temperature and a significant magnetic moment [4] and many of them were predicted to be half-metallic [5,8–11]. Miura *et al* [12] found that Co-based Heusler alloys exhibit over 70% spin polarization. These materials include Co_2CrAl (99.9%), Co_2CrSi (100%), Co_2CrGa (93.2%), Co_2CrGe (99.8%), Co_2MnSi (100%) and Co_2FeAl (86.5%).

Operation of spintronic devices should be avoided at too low temperature; however, many half-metallic systems exhibit a dramatic suppression of spin polarization well below room temperature [2–13]. The electronic correlation seems to play a crucial role in depolarization effects by introducing incoherent nonquasiparticle (NQP) states just above the Fermi level in the minority spin channel [14–16], which are connected with spin-polaron processes. The existence of the NQP states was reported in the Co_2MnSi-based tunnel junctions [17]. To eliminate the NQP states, it is necessary to suppress finite-temperature magnonic excitations, preserving at the same time the minority spin gap. Attema *et al* [18] proposed to increase the magnetic anisotropy and thus the magnon gap by doping with rare-earth atoms in the half-metallic material. For $NiMn_{1-x}RE_xSb$ compounds with RE = Nd, Pm, Ho and U [2,19], it was reported that the half-metallic gap is not affected and that large 3d–4f coupling is obtained in the case of Nd substitution. Burzo *et al* [20] used the linear muffin-tin orbital (LMTO) method within the LDA+U, with effects of doping of holmium impurities into the full-Heusler FM alloy CoMnSi. Their experimental results and theoretical calculations showed that substituting Ho on Co sites introduces finite densities of states (DOS) in the minority spin gap, while substitution on the Mn sites preserves the half-metallic character. Grasin *et al* [21] reported experimental and theoretical studies on the effect of Gd impurity on the physical properties of the Co_2MnSi, and showed that the half-metallic properties are completely conserved if Gd substitutes Mn atoms.

In this work, we study the effect of gadolinium substitution on the physical properties of Co_2CrSi-based alloy. The substitution of Gd in both Co or Cr lattice sites is analysed. The magnetic properties and band structures of the doped compounds are studied.

2. Computational details

The electronic structure calculations are based on the density-functional theory in the local spin-density approximation (LSDA) with an additional Hubbard correlation term that describes on-site electron–electron repulsion associated with

the 4f narrow bands (LSDA+U approach) [22,23]. The first-principle band-structure approach applied in this work is the scalar relativistic full-potential linear-augmented-plane wave plus local orbital (FPLAPW+lo) method [24,25] (Wien2k implementation [26]).

For Co_2CrSi, we used the standard representation of $L2_1$ structure with four interpenetrating face-centred-cubic (fcc) sublattices. Two of the sublattices are equally occupied by Co and combine to form a simple cubic sublattice. The atomic positions are (0, 0, 0) for Co1, (1/2, 1/2, 1/2) for Co2, and (1/4, 1/4, 1/4) and (3/4, 3/4, 3/4) for Cr and Si, respectively, where Co1 and Co2 sites are equivalent. The Gd-doped Co_2CrSi was modelled using a 32-atom supercell of $2 \times 2 \times 2$ constructed using the primitive unit cell. The atomic structure is shown in figure 1. The Co/Cr3d and RE 5p 4f electrons are explicitly treated as valence electrons. We have used muffin-tin radii of 2.2 Bohr for both Co and Cr and 2.3 and 2.0 Bohr, respectively, for Gd and Si, respectively. In the total-energy calculation, the factor $R_{\mathrm{mt}}k_{\mathrm{max}}$ is chosen to be 8.5. The Brillouin-zone integrations were performed using $5 \times 5 \times 5$ Mokhorst–Pack special k-points [27].

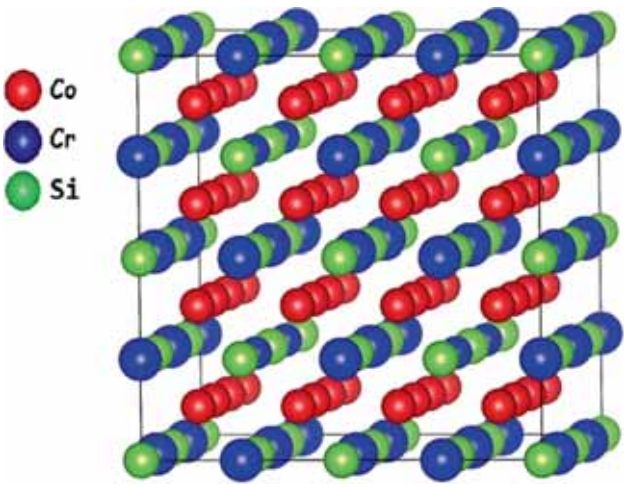

Figure 1. The atomic structure of $Co_{16}Cr_8Si_8$.

3. Results and discussion

Using the experimental lattice constant of 5.65 Å [28] for Co_2CrSi within the LSDA, we calculate the energy band structure as shown in figure 2. The spin direction is taken as the direction of the rare-earth spin (↑ for majority spin direction and ↓ for minority spin). All energies are relative to the respective Fermi level. According to figure 2, the Fermi energy E_F lies in the pronounced gap of the minority-spin states, determining the half-metal character of this compound. The bandgap is estimated to be 0.56 eV. Our results agree well with earlier DFT studies [9,29,30]. Figure 3 exhibits the partial DOS of Co_2CrSi. We report a large DOS of the majority spins at Fermi energy of $N(\uparrow, E_F) = 0.66$ states eV^{-1} $spin^{-1}$ $atom^{-1}$. This is related to the fact that the E_F cuts through localized states of mostly Cr-d-like character as shown in figure 3. The Co-d states contribute fairly to $N(\uparrow, E_F)$. In agreement with previous calculation [29,30], an integer total magnetic moment of 4.00 μ_B is obtained. We also fully optimize the Co_2CrSi crystal structure and report a lattice parameter of 5.52 Å, which is slightly underestimated in comparison with the experimental one estimated by linear extrapolation using the concentration dependence [28]. Calculations with the inclusion of Hubbard potential (LSDA+U) of the properties of the Co_2CrSi [29] have been performed by Rai *et al* [29]. Except the overestimated lattice parameter (of 5.699 Å), only small qualitative changes were reported in the band structure and DOS. Hence, the LSDA gives a good description of the properties of the Co_2CrSi, which is not the case of the rare earths, where the LSDA is not suitable to describe strong correlation of the 4f states.

To simulate the doping of the Co_2CrSi by gadolinium, we have performed calculations using supercells containing 32 atoms. We study the electronic structure of the $Co_{16}Cr_7GdSi_8$ supercell to simulate Gd substitution at the Cr sites and for $Co_{15}GdCr_8Si_8$ cell when Gd replaces Co. In order to investigate the sensitivity of the results with respect to the Coulomb interaction parameter U, we have performed calculations by varying $U-J$ from 7 to 12 eV. For all values, half-metallic characters are obtained. The variation

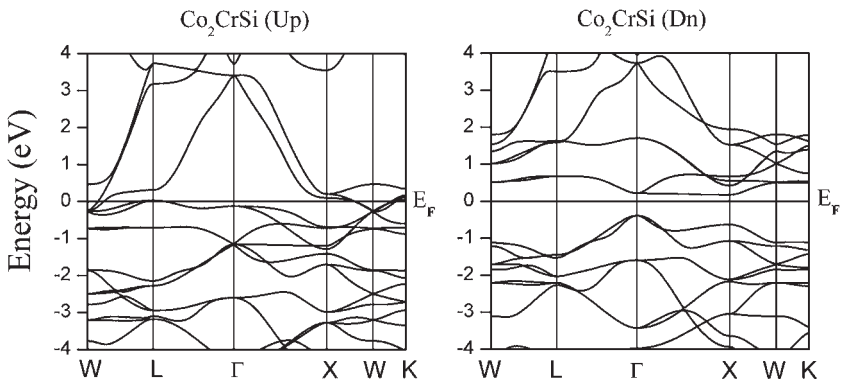

Figure 2. Spin-polarized band structure of Co_2CrSi using LSDA.

of the difference between the bottom of the conduction band (E_b) and the Fermi level, E_b–E_F, with the Gd spin moments as a function of the average Coulomb parameter is given in figure 4. No significant dependence in the studied range of the U parameter was reported: The maximum E_b–E_F difference is on the order of 8 meV and the magnetic moment varies slightly from 6.91 to 6.97 μ_B. Therefore, in our calculations we choose the value of 7 eV for the U–J parameter.

The calculations were done considering a FM and an antiferromagnetic (AFM) coupling of Gd(4f) and Cr/Co(3d) spins. The calculated DOS of $Co_{16}Cr_7GdSi_8$ and $Co_{15}GdCr_8Si_8$ for both FM and AFM coupling are presented in figures 5 and 6, respectively. For $Co_{16}Cr_7GdSi_8$ (figure 5), the half-metallic state is stable in both cases with a bandgap of 0.5 eV magnitude with the Fermi level, which moves slightly towards the valence band. We also note that the behaviour of DOS near E_F is very similar to the undoped case (figure 5), and that Gd(4f) orbitals do not hybridize with the 3d orbitals near E_F; hence, the nature of the carriers around E_F is not changed. The half-metallic properties are completely conserved if gadolinium atoms substitute the chromium atoms. This effect is determined through the coupling between the Gd(4f) spin and the Cr(3d) itinerant electron spins. We evaluate such a coupling by calculating the total energy of compound for a parallel and antiparallel f–d coupling [20]. Given the geometry of the cell, when Gd is substituted into

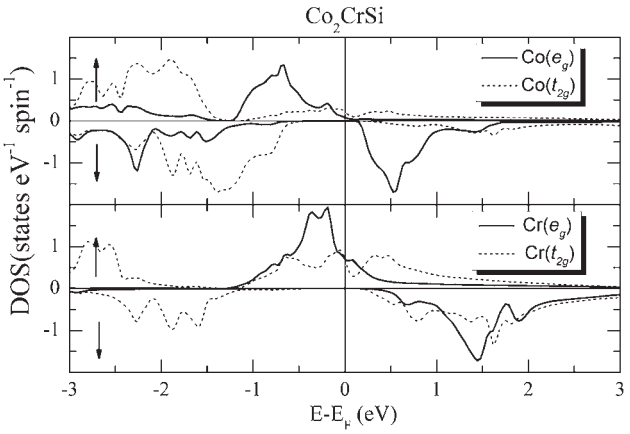

Figure 3. Projected densities of states of the Co_2CrSi Heusler alloy obtained by LSDA.

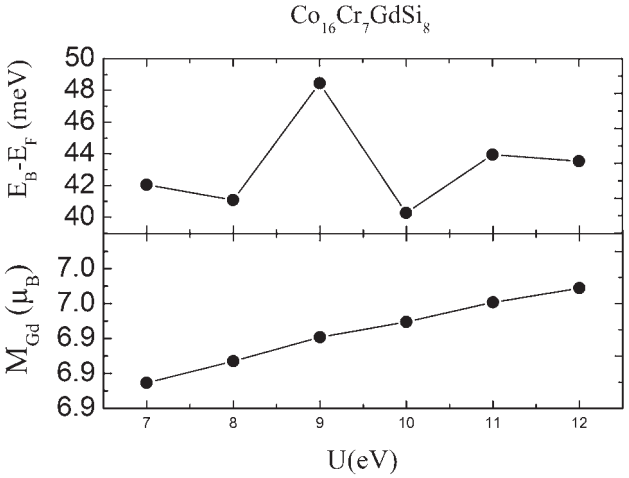

Figure 4. The minority spin half-metallic gap and magnetic moment of Gd as a function of the average Coulomb parameter U.

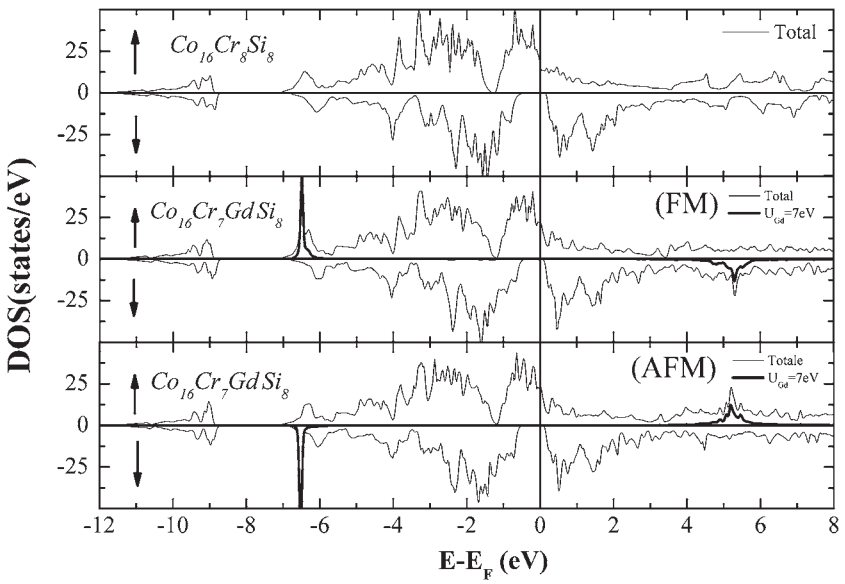

Figure 5. Densities of states of the $Co_{16}Cr_7GdSi_8$ supercell with the ferromagnetic (FM) and antiferromagnetic (AFM) coupling of Gd4f and Cr3d spins. For comparison, the Co_2CrSi densities of states using the same supercell are also plotted.

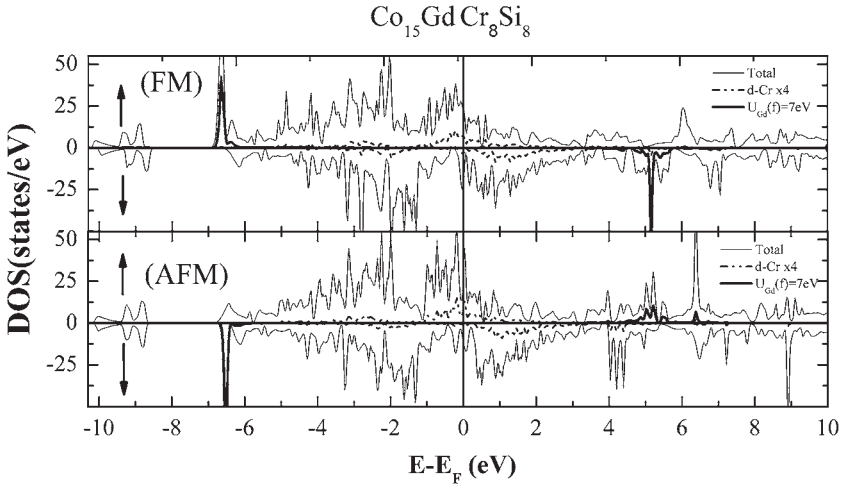

Figure 6. Densities of states of the $Co_{15}GdCr_8Si_8$ supercell with the FM and AFM coupling of Gd4f and Co3d spins.

Table 1. Calculated partial and total magnetic moments for $Co_{16}Cr_8Si_8$, $Co_{16}Cr_7GdSi_8$ and $Co_{15}GdCr_8Si_8$ compounds, in the case of ferromagnetic coupling (FM) and antiferromagnetic coupling (AFM) (the additional Hubbard correlation term is used only for the rare-earth 4f–Gd states).

		Calculated magnetic moments (μ_B)					
Compounds	Magnetic coupling	M_{Co}	M_{Cr}	M_{Gd}	M_{Si}	M_{tot}	E_{tot} (eV)
$Co_{16}Cr_8Si_8$		1.01	1.91	—	−0.02	32	−65924.3736
$Co_{16}Cr_7GdSi_8$	FM	0.99	1.96	6.91	−0.02	35.99	−86372.4636
$Co_{16}Cr_7GdSi_8$	AFM	0.99	1.97	−7.03	−0.03	21.98	−86372.4698
$Co_{15}GdCr_8Si_8$	FM	0.86	1.70	7.04	−0.02	40.47	−105450.8702
$Co_{15}GdCr_8Si_8$	AFM	0.98	1.66	−7.01	−0.03	21.04	−105450.8933

the Cr sublattice, 12 pairs of Gd(4f)–Cr(3d) are formed [20]; thus, the f–d coupling constant is calculated as the $E_{FM}-E_{AFM}$ energy corresponding to a pair. The value of this, with the calculated magnetic moments, is given in table 1. The ΔE energy is estimated to be 71.95 K, with the minimum in the case of AFM coupling between Cr(3d) and Gd(4f) spins. The stability of the AFM phase was reported experimentally and theoretically for Co_2MnSi doped by Ho [20], and theoretically for Gd-doped Co_2MnSi [21]. Our ΔE value is close to that calculated for $Co_{16}Mn_7GdSi_8$ using the FPLMTO within the LSDA+U [21], where similar properties are reported. The resulting total magnetic moments of the supercell were 35.99 μ_B for FM coupling and 21.98 μ_B for AFM coupling. A small negative moment was found on silicon due to the hybridization effects.

In the case of $Co_{15}GdCr_8Si_8$ supercell, the DOS (figure 6) show that the substitution at Co sites fills the minority spin gap for both FM and AFM coupling of Gd(4f) and Co(3d) spins. In addition, in this case the antiparallel configuration is the most stable one (table 1). The occupied Gd(4f) states are located around −6.5 eV and the unoccupied ones are around 5 eV and show no significant contribution around the Fermi level. For total magnetic moment, we report values of 40.47 μ_B for FM coupling and 21.04 μ_B for AFM coupling. A small and negative moment is also induced on silicon, due to the hybridization effect, with a value of −0.02 μ_B. Finally, we report that the metallic AFM $Co_{15}GdCr_8Si_8$ is lower in energy than the half-metallic AFM $Co_{16}Cr_7GdSi_8$ (table 1).

4. Conclusion

Electronic structure and magnetic properties of the Heusler half-metallic ferromagnet Co_2CrSi doped by Gd have been investigated, taking into account the strong correlation of the RE f-electrons using the LSDA+U approach. The results show that the AFM configuration is the most stable one when Gd substitutes the Cr and Co sites. Based on the electronic structure calculation results, substituting Gd on Cr sites preserves the half-metallic character while substitution on the Co sites introduces finite DOS in the minority spin gap.

References

[1] de Groot R A, Mueller F M, van Engen P G and Buschow K H J 1983 *Phys. Rev. Lett.* **50** 2024

[2] Katsnelson M I, Irkhin V Y, Chioncel L, Lichtestein A I and de Groot R A 2008 *Rev. Mod. Phys.* **80** 315

[3] Schwarz K 1986 *J. Phys. F Met. Phys.* **16** L211

[4] Brown P J, Neumann K U, Webster P J and Ziebeck K R A 2000 *J. Phys. Condens. Matter* **12** 1827

[5] Galanakis I and Dederichs P H 2002 *Phys. Rev. B* **66** 174429

[6] Jeng H-T and G Y Guo 2003 *Phys. Rev. B* **67** 094438

[7] Wang Y K and Guo G Y 2006 *Phys. Rev. B* **73** 064424

[8] Kübler K, Fecher G H and Felser C 2007 *Phys. Rev. B* **76** 024414

[9] Kandpal H C, Fecher G H and Felser C 2007 *J. Phys. D Appl. Phys.* **40** 1507

[10] Tung J C and Guo G Y 2013 *New J. Phys.* **15** 033014

[11] Rai D P, Shankar A, Sandeep D N, Singh L R, Sharma B I, Ghimire M P *et al* 2014 *J. Phys. Sci.* **25** 45

[12] Miura Y, Nagao K and Shirai M 2004 *Phys. Rev. B* **69** 144413

[13] Dowben P A and Skomski R 2003 *J. Appl. Phys.* **93** 7948

[14] Chioncel L, Katsnelson M I, de Groot R A and Lichtenstein A I 2003 *Phys. Rev. B* **68** 144425

[15] Chioncel L, Arrigoni E, Katsnelson M I and Lichtenstein A I 2006 *Phys. Rev. Lett.* **96** 137203

[16] Chioncel L, Mavropoulos Ph, Lezaic M, Blügel S, Arrigoni E, Katsnelson M I *et al* 2006 *Phys. Rev. Lett.* **96** 197203

[17] Chioncel L, Sakuraba Y, Arrigoni E, Katsnelson M I, Oogane M, Ando Y *et al* 2008 *Phys. Rev. Lett.* **100** 086402

[18] Attema J J, Fang C M, Chioncel L, de Wijs G A, Lichtenstein A I and de Groot R A 2004 *J. Phys. Condens. Matter* **16** S5517

[19] Chioncel L 2004 Ph.D. thesis (Nijmegen: University Nijmegen)

[20] Burzo E, Balazs I, Chioncel L, Arrigoni E and Beiuseanu F 2009 *Phys. Rev. B* **80** 214422

[21] Grasin R, Vinteler E, Bezergheanu A, Rusu C, Pacurariu R, Deac I G *et al* 2010 *Acta Phys. Pol. A* **118** 648

[22] Anisimov V I, Zaanen J and Andersen O K 1991 *Phys. Rev. B* **44** 943

[23] Anisimov V I, Solovyev I V, Korotin M A, Czyzyk M T and Sawatzky G A 1993 *Phys. Rev. B* **48** 16929

[24] Wimmer E, Krakauer H, Weinert M and Freeman A J 1981 *Phys. Rev. B* **24** 864

[25] Jansen H J F and Freeman A J 1984 *Phys. Rev. B* **30** 561

[26] Blaha P, Schwarz K, Madsen G K H, Kvasnicka D and Luitz J 2001 *WIEN2k: an augmented plane wave + local orbitals program for calculating crystal properties* (Austria: TechnischeUniversität Wien)

[27] Monkhorst H J and Pack J D 1976 *Phys. Rev. B* **13** 5188

[28] Umetsu R Y, Okubo A, Xu X and Kainuma R 2014 *J. Alloys Compd.* **588** 153

[29] Rai D P, Sandeep, Ghimire M P and Thapa R K 2011 *Bull. Mater. Sci.* **34** 1219

[30] Chen X-Q, Podloucky R and Rogl P 2006 *J. Appl. Phys.* **100** 113901